

# A Fuzzy Logic Control Scheme for Electric Automotive Water Pumps

Jibril Abdullahi Bala  
Department of Mechatronics  
Engineering  
Federal University of Technology,  
Minna  
Minna, Nigeria  
jibril.bala@futminna.edu.ng

Ndukwe Okpo Kalu  
Department of Electrical and  
Electronics Engineering  
Nile University of Nigeria  
Abuja, Nigeria  
obinnandukwe60@yahoo.com

Suleiman U. Hussein  
Department of Electrical and  
Electronics Engineering  
Nile University of Nigeria  
Abuja, Nigeria  
elsuligh@gmail.com

Taliha Abiodun Folorunso  
Department of Mechatronics  
Engineering  
Federal University of Technology,  
Minna  
Minna, Nigeria  
funso.taliha@futminna.edu.ng

**Abstract**— The use of electric vehicles (EV) is gradually gaining acceptance over the Internal Combustion (IC) vehicles owing to the need to do away with fossil fuels and their attendant global warming issues. Furthermore, the use of these vehicles calls for an additional mechanism for its cooling as compared to those obtainable on the conventional IC Engines. Electric Automotive Water Pumps (AWP) have been adopted in EHV to replace the belt-driven pumps systems in IC engines. However, the control of these AWP has remained a challenge as the existing control schemes result in fixed gain, thus making it difficult for dynamic vehicle conditions as it may result in overheating conditions. Thus, to address the issues associated with the fixed gain, this paper proposes the use of a fuzzy logic-based controller (FLC) to control the AWP in EVs. The proposed FLC offers an intelligent and adaptive control strategy for the AWP. Furthermore, the performance of the proposed FLC outweighs that of the conventional PID when compared showing no overshoot and providing successful tracking. Thus, depicting that the FLC can be adopted for EVs.

**Keywords**—Automotive Water Pump, Cooling System, Electric Vehicles, Fuzzy Logic Control, PID Control

## I. INTRODUCTION

Owing to the advancement in technology and climate change-related issues, electric vehicles (EV) are gradually being adopted as compared to conventional internal combustion (IC) engine vehicles all over the world [1]. The cooling mechanism in the vehicle remains the most critical component of any vehicle as it is responsible for maintaining the internal temperature to the desired level else overheating conditions are experienced. The Cooling system in the conventional IC engine is often described as the belt-driven mechanical pump system [2]. These pumps are characterized by the engine-dependent speed and the torque required to achieve the desired cooling levels in IC engines. Hence, for effective cooling to be achieved the engine needs to supply a corresponding amount of torque to the pump system to maintain the engine temperature else an overheating is

experienced. Contrarily, in EVs, the cooling systems are achieved using single or multiple electric Automotive Water Pumps (AWPs). Characteristically, these pumps differ from those of the IC engine cooling systems as they depend solely on electric signals for their cooling operations as compared to the torque in the IC-based engines. Furthermore, the AWP cooling system has an edge over the conventional system in its ability to offer faster cooling with less energy consumption and consists of less friction-based parts. Since most AWP is built using Brushless Direct Current (BLDC) motors, hence there is a need for an effective and efficient mechanism to control the speed for improved efficiency.

Some control schemes have been implemented for the control of BLDC motors and other associated electromechanical systems, however, only a few have been implemented for AWP. The Proportional-Integral-Derivative (PID) control scheme remains one of the most popular and widely used control schemes owing to the ease of tuning [3]. This characteristic advantage of the PID makes it a candidate solution in AWP control. However, the dynamic nature of the operation of the AWP in EV systems and the fixed gain characteristics of the PID control make its application challenging as EVs' scenarios of operation are constantly changing [4].

Hence, to accommodate for these changing features of the EVs and consequently the AWP, there is a need for the development of a suitable controller with high performance and robustness to accommodate these dynamic features. In this work, the Fuzzy Logic Controller (FLC) has been proposed for adoption to control the AWP owing to its inherent characteristics of ease of development, and wider operating range [5]. The FLC is also known to achieve a higher degree of trajectory and stabilization as compared to conventional PID controllers [6]. Hence, the basis for the adoption is to provide efficient control performance for the AWP.

The rest of this paper is divided into four parts. Part II presents a review of related works while the research methodology is presented in part III. The results and discussion is presented in part IV while the conclusion is presented in Part V.

## II. LITERATURE REVIEW

The Proportional-Integral-Derivative (PID) controller is a feedback control scheme that is popularly implemented in the control industry. Its high demand stems from its ability to control a wide range of industrial applications such as electromechanical systems, flight control systems, automotive systems, and robotics. PID controllers are implemented in numerous control loops due to their structural simplicity and robustness [7].

On the other hand, Fuzzy Logic Control is frequently seen as a substitute for PID control. This is because using membership functions and rules in parameter selection makes it easier to account for non-linearities and additional input signals in control schemes. Fuzzy Logic Controllers are effective in linear and non-linear applications, thus making them popular in industrial applications [8].

There exist some research on the control of electromechanical systems. However, with little focus on the control of AWP. In [9], Proportional Integral Derivative (PID) and Linear Quadratic Regulation (LQR) controllers were implemented to electronically control an automotive engine cooling system. The results showed that the controllers successfully preserved the engine coolant temperature to reference temperatures with small percentage deviations during different operating conditions. However, the fixed-gain traits of these controllers make them unsuitable for dynamic conditions associated with vehicles.

Furthermore, a demand-based control system was designed for efficient heat pump operations of EVs [10]. The scheme utilized PI schemes for different levels of the system. The results showed that by implementing the proposed demand-based control strategy, the total energy consumption of the pumps and compressor could be reduced by up to 34%. However, the limitations associated with the conventional PI control design apply here.

In addition, an intelligent heat pump air conditioning control system for electric vehicles was developed in [11]. The study implemented a fuzzy logic controller to regulate a heat pump air conditioner. However, no extensive testing or comparative analysis was carried out to ascertain the performance of the technique.

Furthermore, [12] developed sensorless electronic water pumps for automobiles. In the study, the control mechanism employed a sensorless magnetic field-oriented control (FOC) scheme with a sliding mode observer (SMO). To estimate rotor velocity/position, a novel SMO and the phase-locked loop (PLL) were used. These schemes also help to reduce chattering. Similarly, [13] developed an adaptive control scheme for electric water cooling pump sensitivity. The technique used a sensitivity filter to minimize a cost function. Simulation results showed good tracking and disturbance rejection results.

A brushless DC (BLDC) motor drive was developed for automotive water pump systems in [2]. The system utilized a PI controller to regulate a BLDC motor. On one hand, the results showed the validity and quality of the reported designs, and the motor and drive exhibited an efficiency of 78% at the

point of rated torque, 450mNm. On the other hand, the fixed-gain characteristics of the conventional PID make it unsuitable for real-time implementation.

From the ongoing, the PID controller is limited in providing satisfactory control performance for the AWP due to the dynamic operational nature of the pumps. Hence, the need to develop a suitable control scheme to handle the dynamic nature of the AWP. Thus, this work proposes the adoption of a Fuzzy Logic Control (FLC) for the AWP. The incorporation of FLC provides an intelligent control technique for the AWP, thereby solving the challenge of the dynamic operating conditions and the issues of fixed gain.

## III. RESEARCH METHODOLOGY

### A. Electric Automotive Water Pump Model Development

The Automotive Water Pump is modeled as an electromechanical system as shown in Fig. 1 and the parameters used for the AWP are presented in Table I.

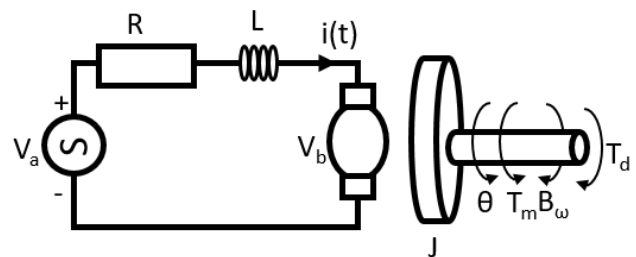


Fig. 1: An Electromechanical System

TABLE I. SYSTEM PARAMETERS OF THE AWP

Parameter	Value
Torque Constant, $K_t$	3.5 NM/Amp
Back EMF constant, $K_b$	3.5 V/rad/sec
Viscous friction coefficient, $B$	0.0348 MN/rad sec
Rotor Inertia, $J$	0.068 Kg/m <sup>2</sup>
Armature Inductance, $L$	0.055H
Armature Resistance, $R_a$	7.56 $\Omega$

For the Electrical Circuit, the sum of voltage drops is given in Equation 1. The parameters  $v_b$ ,  $i_a$ , and  $v_a$  represent back EMF, armature current, and applied voltage respectively.

$$i_a(t)R + L \frac{di_a(t)}{dt} + v_b(t) = v_a(t) \quad (1)$$

Transforming into Laplace, we obtain equation 2.

$$I_a(s)R + LSI(s) + V_b(s) = V_a(s) \quad (2)$$

The torque–armature current relationship is given in Equation 3.  $T_m$  represents the motor torque.

$$T_m(s) = k_t I_a(s) \quad (3)$$

The back EMF – angular velocity relationship is given as shown in Equation 4. The variable  $\Omega$  represents the angular velocity.

$$V_b = k_b \Omega(s) \quad (4)$$

As for the Mechanical Circuit, the torque is related to the rotor inertia and viscous friction coefficient by Equation 5.

$$T_m(s) = JS\Omega(s) + B\Omega(s) \quad (5)$$

Substituting the values for the armature current, motor torque, and back-EMF, we obtain Equation 6, and simplifying, we obtained Equations 7 and 8.

$$\frac{(R+LS)(JS+B)\Omega(s)}{k_t} + k_b\Omega(s) = V_a(s) \quad (6)$$

$$\Omega(s) \left( \frac{(R+LS)(JS+B)}{k_t} + k_b \right) = V_a(s) \quad (7)$$

$$\frac{\Omega(s)}{V_a(s)} = \frac{1}{\frac{(R+LS)(JS+B)}{k_t} + k_b} \quad (8)$$

Therefore, the transfer function model is evaluated as shown in Equation 9.

$$G_s(s) = \frac{\Omega(s)}{V_a(s)} = \frac{k_t}{(R+LS)(JS+B)+k_t k_b} \quad (9)$$

Substituting the following values presented in Table I into the transfer function we obtain the model in Equation 10.

$$G_s(s) = \frac{3.5}{0.004s^2 + 0.5s + 12.3} \quad (10)$$

**B. Fuzzy Logic Control System Design**

In this work, the Mamdani type of fuzzy logic has been adopted because it is well suited to human inputs as compared to others [14]. Furthermore, the proposed fuzzy logic has 3 major components namely: the input fuzzifier, the inference system and rules, and output. The fuzzifier comprises of the parameters selected to serve as input to the inference system. These parameters namely the error and error change are fed into the inference system in their crisp form for fuzzification. The inference system on the other hand maps these inputs are mapped to their equivalent linguistic variables using appropriate membership functions. Furthermore, the fuzzy logic control decision takes place in the inference system using the knowledge-based rules. The output from this process is thereafter defuzzified, thereby converting it back to crisp value for the control operation, this happens at the output stage of the fuzzy logic process. The block diagram of the fuzzy logic control system in relation to the AWP is depicted in Fig. 2.

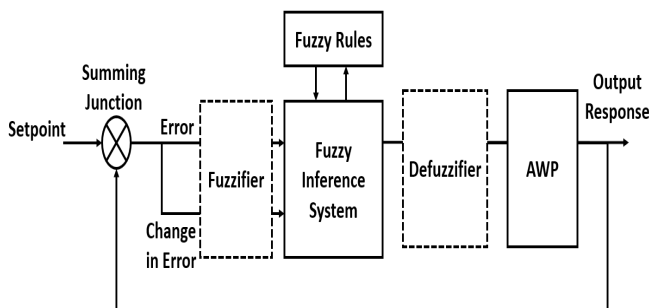


Fig. 2: Fuzzy Logic Control Scheme

The MATLAB's fuzzy logic toolbox (R2021b) was adopted to create the Fuzzy Inference System (FIS). The FIS has two inputs which are the error and error change, and one output, which represents the control signal. The Membership Functions (MFs) were designed using triangular MFs. The

inputs had three MFs each, namely: Negative (neg), Zero (zer), and Positive (pos). The output had three MFs each namely: Big (big), Medium (med), and Low (low). Figs. 3 to 5 show the designed MFs.

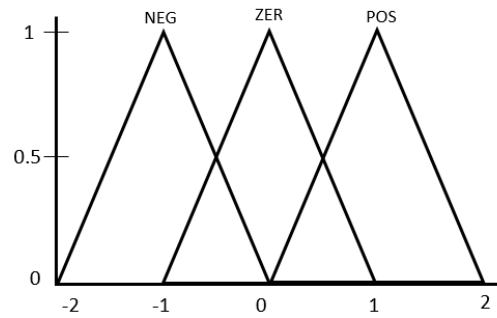


Fig. 3: Membership Function for Error

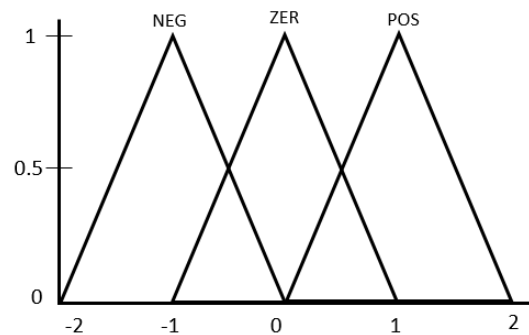


Fig. 4: Membership Function for Change in Error

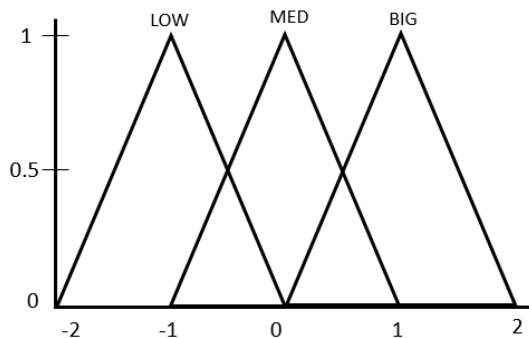


Fig. 5: Membership Function for Change in Control

Some conditions were used to develop the fuzzy rules. First, if the error is small and the rate of error change is slow, keep the current control output. Furthermore, if the error is not zero but the rate of change is approaching zero, keep the current control output. Finally, if the error is greater than zero and the rate of change is decreasing, adjust the control output proportionally to the magnitude of the error. Based on these conditions, the rules were developed as shown in Table II. The surface diagram which shows the relationship between the inputs and the output is presented in Fig. 6.

TABLE II. FUZZY LOGIC CONTROL RULES

e / Δe	N	Z	P
N	N	N	Z
Z	N	Z	P
P	Z	P	P

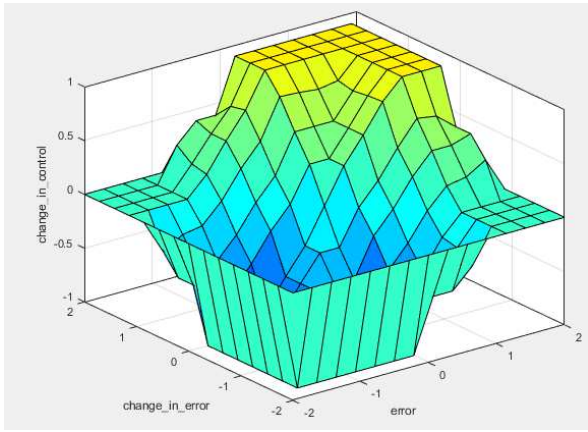


Fig. 6: Surface Diagram for Fuzzy Rules

The centroid method, shown in Equation 11, was used to defuzzify the data. This technique evaluates the area under a curve.

$$R = \frac{\int x\mu_A(x)dx}{\int \mu_A(x)dx} \quad (11)$$

The variables  $x^*$ ,  $x$ , and  $\mu_A$  represent the defuzzified value, sample element, and membership functions respectively.

IV. IMPLEMENTATION, RESULTS AND DISCUSSION

The modelling and simulation of the AWP were achieved using the MATLAB/Simulink (R2021b). The model was simulated using a unit step input, while the performance system was based on the transient response metrics of rise time, settling time, overshoot, and Integrated Absolute Error (IAE) as the performance indices of the controller. The Simulink diagram of the AWP Fuzzy Logic Control is presented in Fig. 7.

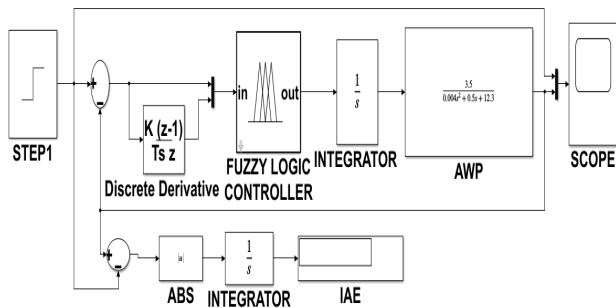


Fig. 7: Simulink Diagram of AWP Fuzzy Logic Control

The structure of the AWP is such that the input signal is fed via a comparator that find the difference between it and the feedback output to give the error signal. The error signal and the differential error signal forms the input to the FLC. These inputs are subjected to the Fuzzy process as highlighted earlier to obtain an output control signal using the rules and the inference system. The output control signal dynamically controls the operation of the AWP based on the created rules as well as the inference system. Based on output control signal the performance plot of the FLC system is as depicted in Fig. 8. Observe from Fig. 8, the system’s open loop response was unable to meet the desired set input and thus exhibiting some undershoot properties which is undesirable to the operations of the AWP. A further analysis of the open loop performance shows an IAE performance of 38.15 which further confirm the need for a suitable controller to improve the performance.

Contrarily, to the open loop performance, the performance of the FLC based controller for the AWP shows significant improvement as compared to that of the open loop in terms of the transient response. The FLC has a rise time and settling time of 10.1sec and 18.7sec respectively. Furthermore, the FLC displayed a zero overshoot which is desirable for the operation of the AWP. In addition, the FLC also has an IAE index of 4.453. In quest to validate the performance of the FLC, a Conventional PID controller was developed for comparison. The performance of the PID controller is also depicted in Fig. 8. The analysis of the PID controller shows a faster response in terms of the rise and settling time to the values of 1.1 secs and 7.7 secs respectively. Characteristically, the response metrics are faster than that of the FLC, however, speed is not desirable in this instance. Furthermore, the FLC has an advantage over the PID controller in terms of overshoot. The PID shows and overshoot of 50.8% which is an undesirable entity in the operations of the AWP.

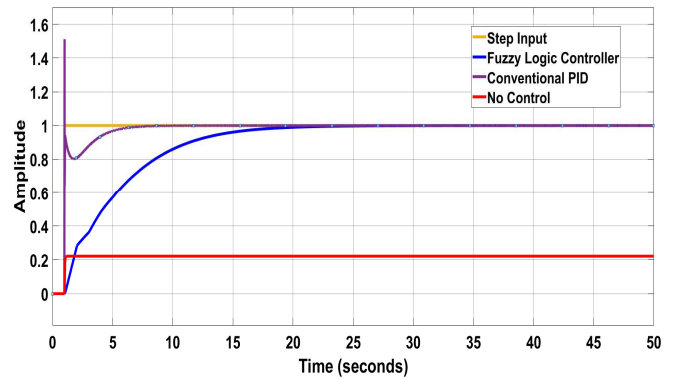


Fig. 8: Comparison of All System Responses

Table III, summarizes the performance metrics of the open loop (No Control condition), the conventional PID and the FLC controllers.

TABLE III. COMPARISON OF CONTROL SYSTEM RESPONSES

Parameter/ Controller	No Control	PID	FLC
Rise Time (secs)	-	1.1	10.1
Settling Time (secs)	-	7.7	18.7
Overshoot (%)	-	50.758	0
IAE	38.15	0.5176	4.453

From the table, it can be observed that although the conventional PID gives a faster response with a lower IAE, it has an overshoot of over 50%. The FLC on the other hand has a slower response, but with no overshoots. These results imply that for applications where the response and performance speed is vital, the PID controller can be used. However, that technique will result in overshoots. On the other hand, if accuracy and effective setpoint tracking is required, the FLC can be used in that case albeit with reduced speed. Of all the three schemes, the technique with no control system gave the worst performance, as it was not able to track the reference signal. In terms of the AWP, the results imply that the PID will provide faster but excessive pumping action, due to the overshoot. On the other hand, the FLC will provide a slower pumping action, but with more accuracy.

## V. CONCLUSION

In this work, a Fuzzy Logic control scheme for electric Automotive Water Pumps (AWPs) in electric vehicles was presented. The technique models the AWP and utilizes a Fuzzy Logic controller to provide an effective control performance of the AWP. The performance of the system is compared with the conventional PID and the results show the effectiveness of the FLC in reference tracking. Although the PID exhibited a faster performance and lower IAE, the FLC was able to minimize the overshoot in contrast to the PID controller which had a high overshoot value. The performance of the system indicates that the scheme can be successfully applied to control AWP in electric and autonomous vehicles. Future research directions will focus on implementing a Fuzzy-PID control scheme for adaptive tuning purposes and comparing the performance with FLC and PID control techniques.

## ACKNOWLEDGMENT

The authors wish to acknowledge the National Information Technology Development Agency (NITDA) for their support through the 2020 NITDEF scholarship scheme.

## REFERENCES

- [1] Y. Liu, Y. Kang, W. Sun, and X. Xu, "Power Control Strategy and Performance Evaluation of a Novel Two-pump Hydraulic Control Unit for BEVs Power Control Strategy and Performance Evaluation of a Novel Two-pump Hydraulic Control Unit for BEVs," 2020.
- [2] J. S. Park, B. Gu, J. Choi, and I. Jung, "Development of BLDC Motor Drive for Automotive Water Pump Systems," *J. Int. Counc. Electr. Eng.*, vol. 1, no. 4, pp. 395–399, 2011.
- [3] H. Yakubu, S. Hussein, G. Koyunlu, E. Ewang, and S. Abubakar, "Fuzzy-PID Controller for Azimuth Position Control of Deep Space Antenna," *Covenant J. Informatics Commun. Technol.*, vol. 8, no. 1, pp. 1–7, 2020.
- [4] H. S. Yakubu, S. Thomas, S. U. Hussein, V. Anye, G. Koyunlu, and O. Oshiga, "Azimuth position control for deep space antenna using fuzzy logic controller," *2019 15th Int. Conf. Electron. Comput. ICECCO 2019*, pp. 31–36, 2019.
- [5] J. A. Bala, O. M. Olaniyi, T. A. Folorunso, and O. T. Arulogun, "Poultry Feed Dispensing System Control: A Case between Fuzzy Logic Controller and PID Controller.," *Balk. J. Electr. Comput. Eng.*, vol. 7, no. 2, pp. 171–177, 2019.
- [6] A. Kosari, H. Jahanshahi, and S. A. Razavi, "An optimal fuzzy PID control approach for docking maneuver of two spacecraft: Orientational motion," *Eng. Sci. Technol. an Int. J.*, vol. 20, no. 1, pp. 293–309, 2017.
- [7] P. Mohindru, G. Sharma, and P. Pooja, "Simulation Performance of PID and Fuzzy Logic Controller for Higher Order System," *Commun. Appl. Electron.*, vol. 1, no. 7, pp. 31–35, 2015.
- [8] E. Yesil, M. Guzelkaya, and I. Eksin, "Fuzzy PID controllers: An overview.," in *The 3rd Triennial ETAI International Conference on Applied Automatic Systems, At Ohrid, Macedonia*, 2003.
- [9] M. Mohamed, M. H. Shedid, M. S. El-Demerdash, and M. Fatouh, "Performance of Electronically Controlled Automotive Engine Cooling System Using PID and LQR Control Techniques," *IOSR J. Mech. Civ. Eng.*, vol. 15, no. 3, pp. 42–51, 2018.
- [10] D. Dvorak, D. Basciotti, and I. Gellai, "Demand-Based Control Design for Efficient Heat Pump Operation of Electric Vehicles," *Energies*, vol. 13, pp. 1–18, 2020.
- [11] L. Zhao, W. Hou, and Q. He, "Intelligent of Electric Vehicle Heat Pump Air Conditioning Control System," *J. Phys. Conf. Ser.*, vol. 2143, pp. 1–5, 2021.
- [12] J. Han, H. Song, C. Feng, X. Zhou, C. Tang, Z. Duan and J. Gao. "Design and Implementation of Sensorless Electronic Water Pump for Automobile," *J. Electr. Electron. Eng.*, vol. 6, no. 1, pp. 31–39, 2018.
- [13] V. V. Kokotovic and C. Buckman, "Electric Water Cooling Pump Sensitivity Based Adaptive Control," *SAE Int. J. Commer. Veh.*, vol. 10, no. 1, pp. 331–339, 2017.
- [14] J. A. Bala, O. M. Olaniyi, T. A. Folorunso, and O. T. Arulogun, "Performance Evaluation of the Effect of Optimally Tuned IMC and PID Controllers on a Poultry Feed Dispensing System," *J. Adv. Comput. Eng. Technol.*, vol. 6, no. 4, pp. 213–226, 2020.